# DISTURBANCE COMPENSATION IN BIPEDAL LOCOMOTION USING GROUND REACTION FORCE FEEDBACK AND THE CMP

Richard Beranek,* Henry Fung,** and Mojtaba Ahmadi*


## Abstract

A novel bipedal locomotion controller based on the centroidal moment pivot (CMP) with ground reaction force feedback is presented. A reference CMP position is planned and a corresponding centre of mass (COM) trajectory is calculated based on the reference CMP. Tracking the reference COM motion results in a net moment acting on the biped that will move the measured CMP to its reference trajectory. This control approach implicitly regulates the angular momentum of the robot under disturbances and increases the robustness of the robot to external disturbances. Dynamic simulation results show that the proposed controller can generate stable walking gaits and increase disturbance robustness by up to 100% compared to a ZMP-based controller.



## Key Words

Bipedal control, centroidal moment pivot


## 1. Introduction

During normal operation, where a humanoid robot interacts with the external environment, the robot will be subjected to many unknown disturbances that can result in a loss of balance. Therefore, it is a key objective to design a bipedal walking controller that can compensate for such disturbances, and do so in real time. Thus far, many controllers have been designed that can generate stable walking gaits based on the zero moment point (ZMP) ground reference point [1]–[6]. Most of these controllers use a simplified model of the robot's dynamics, known as the linear inverted pendulum model [3], [7]. This simplified model can be used to plan walking trajectories in real time; however, it results in many aspects of the robot dynamics to be lost [4]. This model simplification poses difficulty when designing controllers required to compensate for large disturbances. As a result, many researchers have attempted to augment ZMP-based approaches to increase the robustness to external disturbances. Some have implemented more complex pendulum models, used estimators to determine the disturbance being applied [5]–[8] or moved to a different control paradigm such as using central pattern generators [9]. Recent work has examined the potential of using angular momentum regulation as a means of increasing robustness to disturbances [10]–[13]. These approaches are motivated by biomechanical observations of human walking that have shown that angular momentum as well as the rate of change of angular momentum are highly regulated quantities during walking [12], [14]–[16]. Kajita *et al.* [11] developed the resolved momentum control, which directly regulates the linear and angular momenta of the robot. This approach required a complete and accurate model of the robot's dynamics for implementation. Although resolved momentum control showed improved disturbance compensation capabilities, when combined with walking, it was difficult to achieve smooth cyclic walking while completely regulating angular momentum [11]. This has led some to propose controllers where the angular momentum is planned, based on different inertia modelling methods [12]–[14]. A second paradigm has been suggested in which angular momentum does not need to be controlled directly, but, rather, rate of change angular momentum can be regulated. Popovic *et al.* [10], [14] introduced a new ground reference point based on the zero rate of change of angular momentum (ZRAM) called the centroidal moment pivot (CMP). This ground reference point allowed to estimate the net moment acting on the biped using feedback of the ground reaction forces (GRF). The CMP model was validated in human walking trials [15] and control methods to regulate momentum based on the CMP were suggested [12], [14]. Other works have also implemented controllers that regulate the rate of change of angular momentum [17]. However, in these approaches, perfect regulation could not be achieved when external disturbances where acting on the robot.


* Department of Mechanical and Aerospace Engineering, Carleton University, Ottawa, Canada; e-mail: richardberanek@cmail.carleton.ca, Mojtaba.Ahmadi@carleton.ca

** CAE Inc., Montreal, Canada; e-mail: henry.fung@cae.com



*Recommended by Prof. Maki Habib*

*(DOI: 10.2316/Journal.206.2015.3.206-4119)*

This resulted in a build-up of angular momentum which eventually caused the robot to tip over. Therefore, a separate method was used to compensate for the increase in total angular momentum. As in the resolved momentum control approach, this required an accurate model of the robot dynamics or an inertia model.

The controller presented in this paper proposes a novel method of planning centre of mass (COM) motions based on the CMP criterion with GRF feedback. Rather than applying the ZRAM condition directly as in previous works, or regulating the angular momentum directly, the proposed controller regulates angular momentum implicitly while allowing for some variation in the rate of change of angular momentum. This is accomplished by defining a reference CMP trajectory for the robot to follow. Combined with GRF feedback, a reference COM is then calculated which can be tracked using approaches such as Sugihara's whole body cooperative method [18]. With this approach there are two key novel aspects of the proposed controller: (1) the angular momentum of the robot can be regulated implicitly using a concentrated mass model that does not include the robot's inertia and (2) by exploiting the coupling between the COM, CMP and centre of pressure (COP), the robustness to external disturbances is increased compared to an equivalent ZMP-based controller.

## 2. Centroidal Moment Pivot

The CMP is a ground reference point meant to provide a measure of the moments acting on a bipedal system. The CMP was developed as a result of studies into human walking mechanics [10], [12], [14], [15]. These studies showed that total angular momentum was a highly regulated quantity in human walking, and as a result, the rate of change of angular momentum is also highly regulated. In order for the rate of change of angular momentum to remain zero, the net moment acting on the system must be zero. Based on this zero-moment condition, the position of the CMP was defined by Popovic *et al.* [10]. If we consider the free body diagram of a biped, shown in Fig. 1(a), where the only forces acting on the body are the GRF and weight of system acting at the COM; the total moment acting on the system can be expressed as:

$$(X_{COP} - X_{COM}) \times GRF = \frac{dH}{dt} = T \qquad (1)$$

where $X_{COM}$ and $X_{COP}$ are the positions of the COM and COP, respectively, $H$ is the angular momentum about the COM and $T$ is the net moment acting about the COM of the biped. For spin angular momentum to remain zero, resulting in indirect regulation of the total angular momentum, the moment acting about the COM must be equal to zero as:

$$(X_{CMP} - X_{COM}) \times GRF = \frac{dH}{dt} = 0 \qquad (2)$$

Note that in (2) the position of the COP has been substituted by the position of the CMP. This indicates that the CMP position is the point at which the GRF must act to maintain the zero-moment condition described in (2). This condition is illustrated in Fig. 1(b), where a disturbance is applied to the biped. In this case, the line of action of the GRF does not pass through the COM, resulting in a net moment acting on the biped. If the net GRF point of action was located at the CMP, then the line of action of the GRF would pass through the COM satisfying the zero-moment condition. To calculate the position of the CMP, (2) can be broken down for an individual axis as:

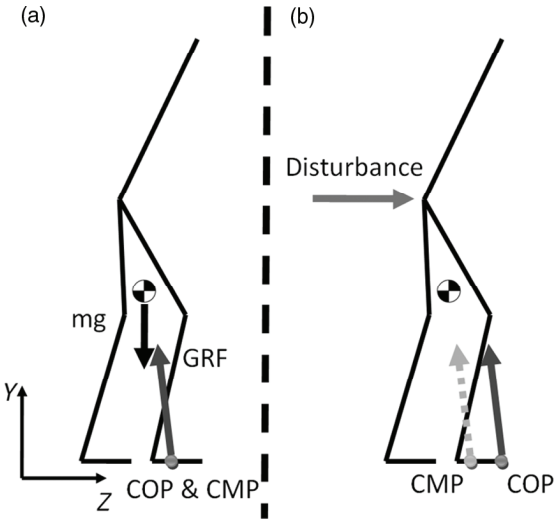


Figure 1. Free body diagram of a bipedal system used to derive the CMP position: (a) no disturbance is present (b) a disturbance generates a net moment and causes the CMP to diverge from the COP.

$$x_{CMP} = x_{COM} - \frac{F_{grx}}{F_{gry}} y_{COM} \qquad (3)$$

where $F_{grx}$, $F_{gry}$ are the GRF for the $x$ and $y$ axes. Hence, to determine the position of the CMP, a measurement or estimate of the GRF, including the shear or lateral forces, is required. In summary, the position of the CMP gives an estimate of the net moments acting on the bipedal system. If the CMP and COP are coincident, then there are no net moments acting on the system. As the COP and CMP diverge, this indicates there is a net moment acting on the system. However, the CMP position was derived assuming that the only forces acting on the system (*i.e.*, no net moments resulting from the disturbance) are the GRF and the weight. If other forces act on the system, such as disturbances, and these forces generate a moment about the COM, then the estimate given by the CMP of the moments acting on the biped may no longer be accurate.

## 3. CMP-based Control Algorithm

As described in Section 2, the CMP provides an estimate of the net moment acting on a bipedal system. Although some small moments are expected during walking, large moments will result from external disturbances. The controller presented in the following section uses the CMP in combination with direct feedback of the GRF to create a

controller that is more robust to these disturbances. As described in the introduction, some previous works have identified the potential to augment robustness to external disturbances using rate of change of angular momentum regulation [17], [19]. However, these works identified that exact regulation of the rate of change of angular momentum is not a possible condition, as described in (2), due to tracking errors and unmodelled moments generated by disturbances. This resulted in a build-up of angular momentum that needed to be regulated using a separate strategy. In the proposed controller, rather than attempting to regulate the rate of change of angular momentum in transience, a reference CMP position, $X_{rCMP}$, is defined and the controller attempts to track the actual CMP position to the reference CMP [20]. This tracking is accomplished by defining a reference COM position, $X_{rCOM}$, as:

$$x_{rCOM} = x_{rCMP} + \frac{F_{grx}}{F_{gry}} y_{COM} \tag{4}$$

$$z_{rCOM} = z_{rCMP} + \frac{F_{grz}}{F_{gry}} y_{COM} \tag{5}$$

for the $x$ and $z$ axes, where (4) and (5) are (3) with the CMP position substituted by the reference CMP. In other words, the reference COM position that is calculated in (4) and (5) is the COM location required such that the CMP will move to the reference CMP, given the measured GRF. The reference CMP is planned to lie within the support polygon of the robot as this is a sufficient, but not necessary, constraint to maintain balance [10]. As a result, the reference CMP matches the walking motion of the robot as a function of the stride length and step time. We must also note that a measurement of the total GRF is required to implement this controller. In practice, this can be achieved by placing a 6-axis force-torque sensor between the ankle and foot of the robot. From these measurements, the COP and lateral forces of the GFR can be estimated.

The expected behaviour of the system is illustrated in Fig. 2. Initially when the robot is disturbed in Fig. 2(a), the CMP will diverge from the COP, indicating that a net moment is acting on the system as a result of a disturbance. In Fig. 2(b), the controller, defines a new reference COM position such that the line of action of the GRF would pass through the reference COM position if the COP moves to the reference CMP position. Note that the reference CMP and actual CMP are not coincident in this transient state. As a result, if the COM tracks the reference COM position defined in (4) and (5), a net moment will be generated that acts to move the CMP and COP towards the reference CMP to achieve the steady-state result, as shown in Fig. 2(c), where all three points are coincident and a new balanced equilibrium is achieved. Given that a net moment is generated by the controller in transience, the zero-moment condition described in (2) is not satisfied and the rate of change of angular momentum is not regulated. However, the generated moment acts to move the CMP to the reference CMP position and counteracts net moments acting on the system. This motion implicitly regulates the total angular momentum. In other words, any build-up of angular momentum in the system is automatically regulated with this control architecture.

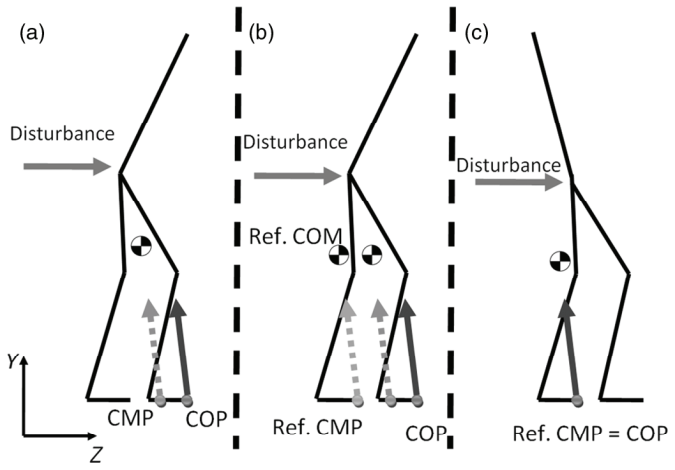


Figure 2. Description of the control algorithm behaviour: (a) undisturbed robot; (b) transient phase when the robot is disturbed and (c) final steady-state posture with disturbance still applied.

### 3.1 COM Tracking Control

The output of the control algorithm specified in (4) and (5) is a reference COM position for the robot to track. Tracking reference COM motions has been used extensively in previous balance controllers based on the ZMP. The tracking controller implemented is based on the whole body cooperative method developed by Sugihara [7], [18]. The first step consists of defining a reference COM velocity, $\dot{X}_{rCOM}$, as:

$$\dot{X}_{rCOM} = K_p e_{COM} + K_d \dot{e}_{COM} \tag{6}$$

where $e_{COM}$ is the error between the reference and actual COM positions; $K_p$ and $K_d$ are diagonal proportional and derivative gain matrices that are tuned heuristically. The reference COM velocity calculated in (6) can be related into individual joint angle velocities, $\dot{\theta}$, using the COM Jacobian, $J_{COM}$, as:

$$\dot{X}_{rCOM} = J_{COM} \dot{\theta} \tag{7}$$

A set of reference joint velocities, $\dot{\theta}_r$, can be calculated by using the inverse relation of (7):

$$\dot{\theta}_r = J_{COM} \dot{X}_{rCOM} \tag{8}$$

where $J_{COM}$ is the pseudoinverse of the COM Jacobian. The joint reference velocity is then integrated to generate a final set of reference joint angles. The resulting control architecture for the CMP-based controller is summarized in the block diagram as shown in Fig. 3. An initial CMP is planned based on the robot gait parameters, such as stride length and time. Although the CMP is not

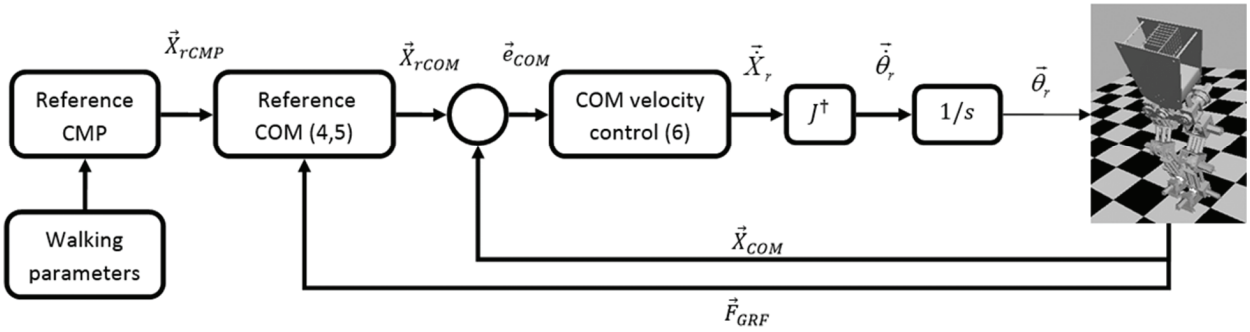


Figure 3. Block diagram of the CMP-based controller.

required to stay within the support polygon to maintain balance [15], it is expected in steady state the COP will be coincident with the reference CMP. Given that the COP must remain within the support polygon to maintain balance, the reference CMP is planned to remain within the support polygon as well. With GRF feedback from the biped, a reference COM position is calculated using (4) and (5). This reference COM position is tracked by decomposing the motion into a set of reference joint angles which are tracked by local joint proportional derivative controllers.

## 4. Simulation Results and Discussion

The proposed controller was implemented in a 3D dynamic simulation of the ABL-BI [21] (Advanced Biomechatronics and Locomotion Laboratory Biped one) robot. Two different conditions are presented: (1) a walking test with no disturbances and (2) balancing on one foot while a disturbance is applied to the robot. The objective of the walking test is to establish if the CMP-based controller, defined by (4) and (5), can generate a stable walking gait. For the second test, we try and establish if using the CMP controller can result in greater robustness to external disturbances.

### 4.1 Simulation Model

ABL-BI has a total of 13 degrees-of-freedom (DOF) as shown in Fig. 4. Each leg has a total of 6 DOF allowing for full 3D motion and an additional DOF is available in the torso to allow for weight shift in the coronal plane. Table 1 contains additional modelling parameters. The dynamic model was built using Simulink$^{TM}$ SimMechanics$^{TM}$ toolbox where mass and inertia parameters for each joint were set to be equivalent to ABL-BI's design. No slip is assumed between the foot and the ground. We believe this to be a reasonable assumption given that the lateral (shear) foot force to normal force ratio does not exceed 0.15. In other words, if coulomb friction is assumed, the static friction coefficient would have to be smaller than 0.15 for slip to occur, which is smaller than the typical range of 0.4–0.6 for a typical foot–floor contact.

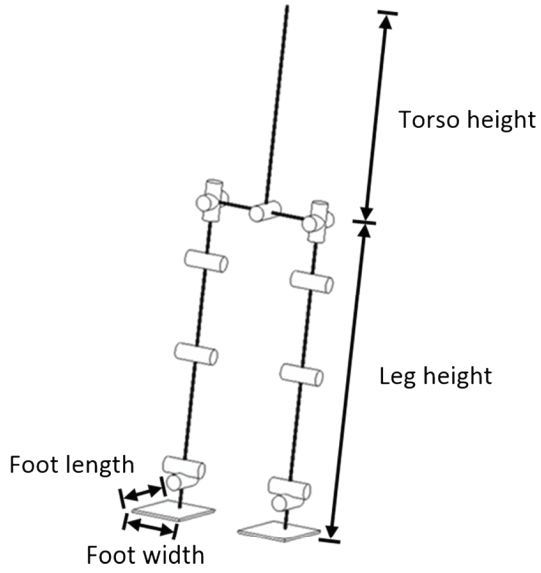


Figure 4. Kinematic structure of the ABL-BI robot.

### 4.2 Walking Results

The first case that was examined using the CMP-based controller was generating a stable walking gait. The gait parameters used for walking are a stride length of 0.1 m, step height of 0.03 m and step time of 2 s. A slower walking speed is required given the mass distribution of ABL-BI, where 80% of the mass is concentrated in the legs. This results in large lateral motions that are required to shift the weight from one foot to another, resulting in limited dynamic walking speeds. A successful walk was generated and results for a 25 step simulation are presented. Figure 5 shows the phase plane for the y-COM motion and a Poincaré map taken at the touchdown of the left foot. The phase plane of the COM motion shows that a stable repetitive cycle is achieved, indicating that the walking motion is stable. This is also reflected in the Poincaré map that shows after the first step, the state of the robot is repetitive within a range of 0.001 m for the COM position and 0.005 m/s for the COM velocity.

As discussed in Section 3, the robot must track a reference COM motion to move the CMP to the reference CMP position. The motion of the COM for one cycle of walking (two steps) is shown in Fig. 6(a). This figure

Table 1
ABL-BI Specifications and Model Parameters

| Height | Leg Length | Torso Length | Foot Length | Foot Width | Control Frequency | Total Mass |
|---|---|---|---|---|---|---|
| 1.0 (m) | 0.6 (m) | 0.4 (m) | 0.15 (m) | 0.10 (m) | 500 (Hz) | 23 (kg) |

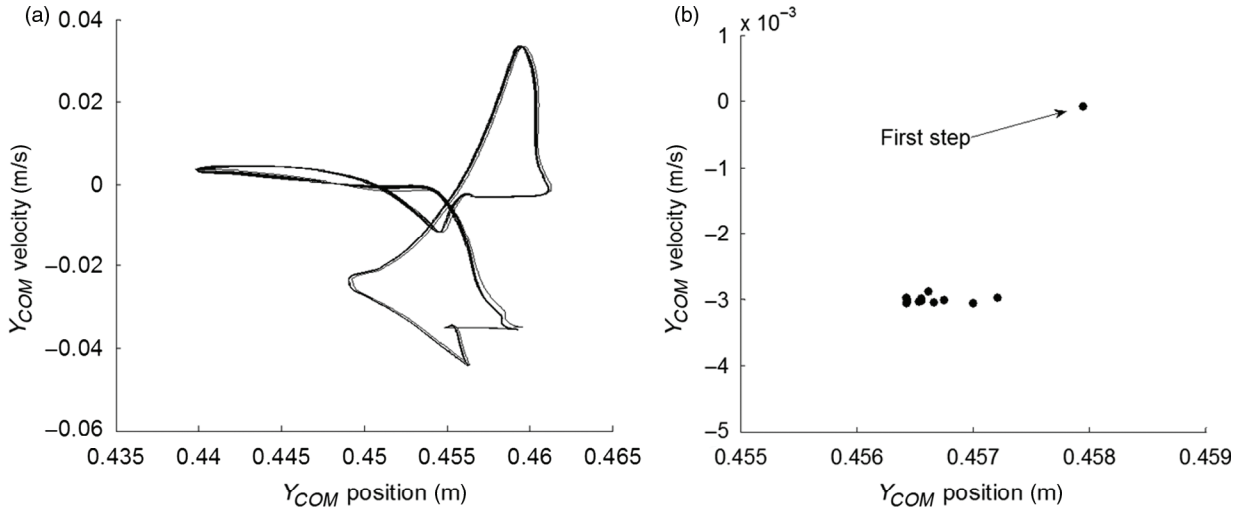


Figure 5. (a) Phase plane of the COM in the $y$-axis and (b) corresponding Poincaré map taken at the touchdown of the left foot.

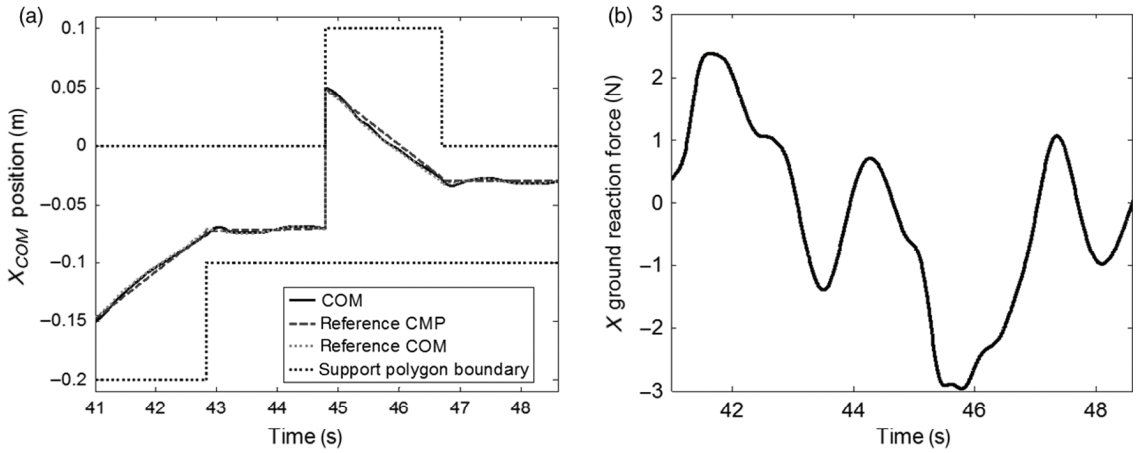


Figure 6. (a) Motion of the COM position in the $x$-axis compared to the reference CMP and COM. (b) Measured GRF in the $x$-axis.

shows that the controller successfully tracks the reference COM motion to within 0.005 m. Also, it can be seen that the planned reference COM trajectory does not diverge by more than 0.01 m from the reference CMP trajectory. Referring back to (4) and (5), this indicates that the net moment acting on the biped is not significant. This is a result of small lateral GRF, as shown in Fig. 6(b) where the lateral GRF does not exceed ±3 N. This result indicates that, during normal walking, the controller essentially behaves as a ZMP-based controller where the robot is following a pre-planned motion based on the reference CMP trajectory.

### 4.3 Disturbance Compensation Results

The second case that was examined consisted of applying a disturbance to the robot while the robot was balancing on one foot. The disturbance was applied to the pelvis and the magnitude of the disturbance in the $x$ and $z$ axes was varied ($y$-axis force was kept zero). Although the disturbance was applied as a pure force in the simulation, the force can be representative of a person pushing the robot, the robot leaning on the environment or the robot making contact with the environment while walking. The objective of this test was to compare the CMP-based controller to

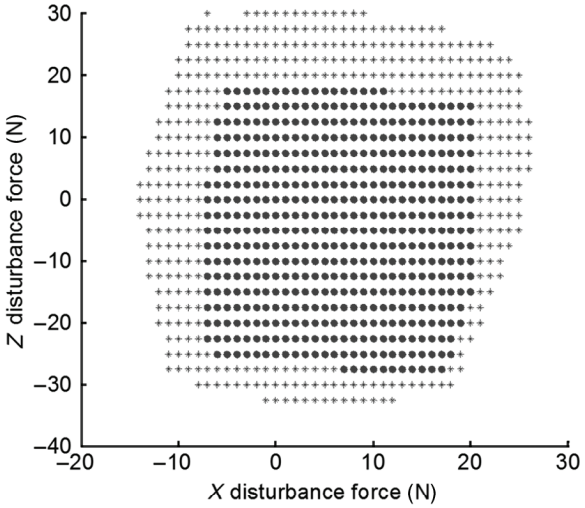


Figure 7. Region showing under which disturbance balance was maintained using the proposed CMP-based controller (blue *) and a standard ZMP-based controller (red •).

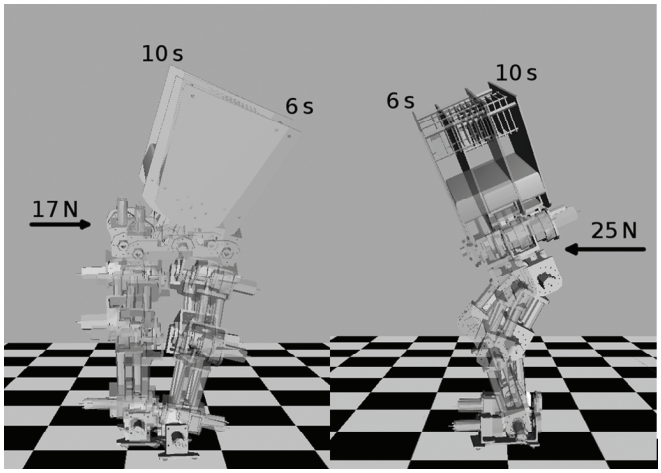


Figure 8. Motion of the simulated robot while balancing on a single foot. A disturbance of 17 N in $x$-axis and 25 N in $z$-axis is applied continuously starting at 6 s. The initial position at 6 s is shown in yellow and final steady-state stance at 10 s in grey.

an equivalent ZMP-based controller based on Sugihara's work in [3]. In both these controllers, a concentrated mass model is used, and the whole body cooperative method is applied to generate desired COM motions. Therefore, the only difference between the two controllers is the method of planning the COM trajectory – CMP or ZMP based. As a result, the comparison suggests whether changing the COM motion alone, based on CMP planning, may improve the balancing abilities of the controller. However, other augmented controllers, such as those based on more complex pendulum models [8], [22], or other balancing strategies such as stepping manoeuvres [23]–[25], may provide greater robustness to external push type disturbances.

The resulting cases, where the controller was able to maintain balance, are plotted in Fig. 7 in blue stars (*). The red circles (•) in Fig. 7 show the conditions under which a ZMP-based controller was able to maintain balance. These results clearly show that the CMP-based controller was able to compensate for larger disturbances and increased the robustness of the controller compared to a ZMP-based controller. The rectangular shape of the region indicates that the robustness to disturbances in the $z$ and $x$ axes are independent. Although the increase in robustness is not uniform under all loading conditions, in the best case, $z$-axis robustness increases by 71% and $x$-axis robustness increases by 100%. Hence, hypothesis (2) from the Introduction is confirmed – the proposed controller is capable of increasing the robustness of the biped to external push disturbances. Applying the disturbance during single stance also presents a worst-case scenario, where the support polygon is at its smallest. Although not presented, similar increases in robustness are also observed if the disturbance is applied during double stance.

For the following results a specific disturbance case is presented, where the magnitude of the disturbance is 17 N in the $x$-direction and 25 N in the $z$-direction. The robot begins in double stance and initiates the pre-planned walking motion, with transition to single stance at 4.9 s, the disturbance is then applied at 6 s and is kept constant afterwards. After the application of the disturbance, the motion of the swing foot is stopped, to force the robot to balance on one foot. The resulting motion of the biped can be seen in Fig. 8 from the time that the disturbance is applied, to when the robot achieves a new equilibrium configuration. Qualitatively, the motion of the biped is to the back and right (in the robots reference frame), to compensate for the disturbance that is pushing the robot forward and to the left. Similarly to the walking experiment, the COM motion can be examined to understand the controller behaviour and is plotted in Figs. 9(a) and 10(a). Both figures show that the reference COM motion is tracked within 0.005 m, indicating that the reference motion is successfully generated during both the transient and steady-state phase. However, unlike the walking test, the reference COM diverges significantly from the reference CMP motion. This shows that the controller is deviating from the pre-planned motion of the robot and generates a new COM trajectory. This is the result of the large lateral GRF shown in Figs. 9(b) and 10(b), which generates a net moment about the COM. For the $x$-axis, the GRF settles to $-17$ and $-25$ N for the $z$-axis; both are equal in magnitude and opposite in direction to the disturbance being applied. These forces generate net moments acting about the COM, causing the reference COM to diverge from the reference CMP as described in (4) and (5). This change in the planned COM motion is the key differentiation between the CMP-based controller and a ZMP-based controller. In a ZMP controller, the planned COM motion would not diverge from the pre-planned motion, given that the planned COM is not modified as a function of the GRF feedback.

The second expected behaviour of the controller is that the measured CMP will track the reference CMP and, in steady state, the COP (note that in Fig. 11, the COP position is also equivalent to the ZMP [4]) will converge

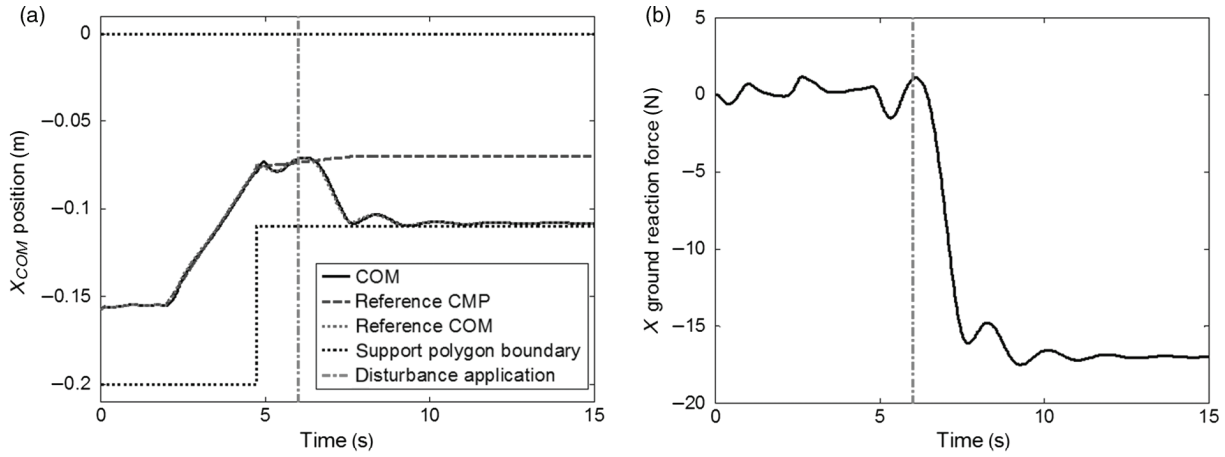


Figure 9. (a) COM motion in the $x$-axis compared to the reference CMP and COM trajectories and (b) measured GRF in the $x$-axis. Shift to single stance occurs at 4.9 s.

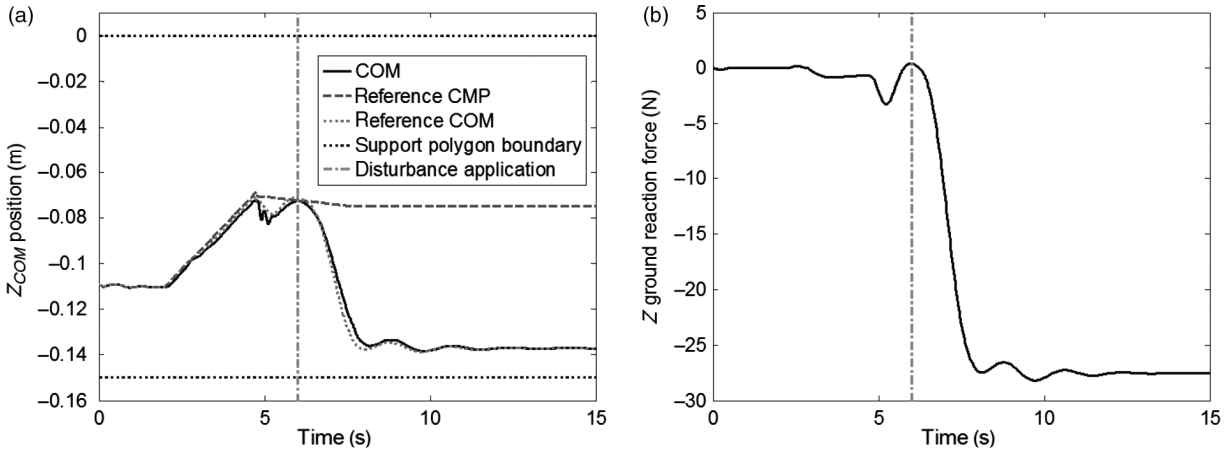


Figure 10. (a) COM motion in the $z$-axis compared to the reference CMP and COM trajectories and (b) measured GRF in the $z$-axis. Shift to single stance occurs at 4.9 s.

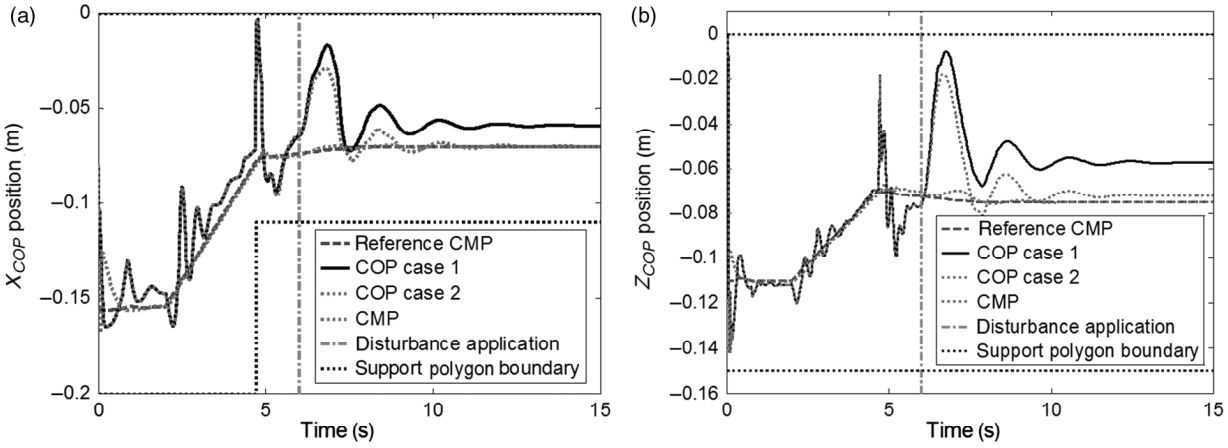


Figure 11. Comparison of the reference CMP, measured CMP and COP for the $x$-axis in (a) and $z$-axis in (b). Case 1 corresponds to a disturbance being applied to the pelvis, 0.09 m above the COM and case 2 corresponds to a disturbance applied directly to the COM. Shift to single stance occurs at 4.9 s.

to the CMP position (both reference and measured). The resulting motion of these points is shown in Fig. 11. For the case where the disturbance is applied to the pelvis (case 1), the actual CMP tracks the reference CMP within 0.003 m; however, the COP does not converge to the reference CMP once steady state is reached, with a steady-state error of 0.012 m in the $x$-direction and 0.018 m in the $z$-direction. This is a result of a moment acting on the biped which is not

accounted for in the controller. As discussed in Section 2, the definition of the CMP only takes into account moments generated by the GRF. The disturbance is applied at the pelvis which is approximately 0.09 m above the COM. Hence, the disturbance generates a moment that is not taken into account in the CMP calculation. Conversely, if the disturbance is applied directly to the COM (case 2) and does not generate a moment about the COM, than the result in Fig. 11 shows that the COP converges to the reference CMP as expected.

During transience, we can see from Fig. 11 that the CMP tracks reference CMP within 0.005 m. This indicates that the condition set in (4) and (5) are satisfied throughout transience as well. In other words, the COM motion prevents the CMP to diverge for the reference CMP significantly, which would cause a large moment to act on the robot. The COP also tracks the reference CMP motion within the transient phase, although there are some peaks where the COP diverges from the reference CMP by up to 0.05 m. These peaks occur during the switch from double to single stance which causes a brief shift in the COP.

The tracking of the reference and actual CMP can also be related to the regulation of angular momentum in the system. As indicated above, the tracking error between both parameters is not exactly zero. This indicates the condition in (2) is not satisfied and the rate of change of angular momentum in the system is not perfectly regulated. However, the planned COM motion indirectly acts to regulate the net angular momentum in the system by generating a restorative moment, causing the CMP to move to the reference CMP in steady state, resulting in a balanced posture.

In summary, the results show that using the GRF feedback with the CMP controller does generate a controller capable of compensating for larger disturbances. However, as the moment arm between the COM and the point of application of the disturbance grows, the estimate of the disturbance becomes less accurate. Despite this inaccuracy in the moment estimate, the controller still improves robustness to the external disturbance compared to a standard ZMP controller.

## 5. Conclusion

The proposed CMP-based controller with GRF feedback was able to generate stable cyclic walking as well as increase the robustness of the controller to external push type disturbances. The results showed that during walking, lateral GRFs remained negligible and the controller operated effectively as a ZMP-based controller. For the test case where the robot was disturbed with a push type disturbance, the GRFs were equivalent to the disturbance being applied and the controller was able to generate a COM motion that moved the CMP to the reference CMP. This suggests that complete GRF feedback can be used to effectively estimate the disturbance applied to the robot, and compensates for the disturbance using a CMP-based control approach. The results also show that although the rate of change angular momentum is not directly regulated by the proposed controller, total angular momentum is implicitly regulated using a concentrated mass model of the robot. However, when the disturbance was not directly applied to the COM, resulting in an additional moment applied to the system, the CMP did not converge to the reference trajectory in steady state. This indicates that as moments resulting from disturbance increase in magnitude, the moment estimate from the CMP position will decrease in accuracy. Future work will focus on evaluating the CMP-based controller on the ABL-BI robot and validating the results observed in the dynamic simulation.

## References


[1] K. Nishiwaki, S. Kagami, J.J. Kuffner, M. Inaba, and H. Inoue, Online humanoid walking control system and a moving goal tracking experiment, *IEEE International Conference on Robotics and Automation*, *1*, 2003, 911–916.

[2] J.I. Yamaguchi, A. Takanishi, and I. Kato, Development of a biped walking robot compensating for three-axis moment by trunk motion, *IEEE/RSJ International Conference on Intelligent Robots and Systems*, *1*, 1993, 561–566.

[3] T. Sugihara, Y. Nakamura, and H. Inoue, Real-time humanoid motion generation through ZMP manipulation based on inverted pendulum control, *IEEE International Conference on Robotics and Automation*, *2*, 2002, 1404–1409.

[4] M. Vukobratovic and B. Borovac, Zero-moment point thirty five years of its life, *International Journal of Humanoid Robotics*, *1*(1), 2004, 157–173.

[5] K. Hirai, M. Hirose, Y. Haikawa, and T. Takenaka, The development of Honda humanoid robot, *IEEE International Conference on Robotics and Automation*, *2*, 1998, 1321–1326.

[6] S. Kajita, O. Matsumoto, and M. Saigo, Real-time 3D walking pattern generation for a biped robot with telescopic legs, *IEEE International Conference on Robotics and Automation*, *3*, 2001, 2299–2306.

[7] T. Sugihara, Mobility enhancement control of humanoid robot based on reaction force manipulation via whole body motion, (Doctoral dissertation, PhD thesis, University of Tokyo), 2004.

[8] J.H. Park and K.D. Kim, Biped robot walking using gravity-compensated inverted pendulum mode and computed torque control, *IEEE International Conference on Robotics and Automation*, *4*, 1998, 3528–3533.

[9] M.K. Habib, K. Watanabe, and K. Izumi, Biped locomotion using CPG with sensory interaction, *IEEE International Symposium on Industrial Electronics*, 2009, 1452–1457.

[10] M.B. Popovic, A. Goswami, and H. Herr, Ground reference points in legged locomotion: Definitions, biological trajectories and control implications, *The International Journal of Robotics Research*, *24*(12), 2005, 1013–1032.

[11] S. Kajita, F. Kanehiro, K. Kaneko, K. Fujiwara, K. Harada, K. Yokoi, and H. Hirukawa, Resolved momentum control: Humanoid motion planning based on the linear and angular momentum, *IEEE/RSJ International Conference on Intelligent Robots and Systems*, *2*, 2003, 1644–1650.

[12] A. Goswami and V. Kallem, Rate of change of angular momentum and balance maintenance of biped robots, *IEEE International Conference on Robotics and Automation*, *4*, 2004, 3785–3790.

[13] S.H. Lee and A. Goswami, Reaction mass pendulum (RMP): An explicit model for centroidal angular momentum of humanoid robots, *IEEE International Conference on Robotics and Automation*, 2007, 4667–4672.

[14] M. Popovic, A. Hofmann, and H. Herr, Angular momentum regulation during human walking: biomechanics and control, *IEEE International Conference on Robotics and Automation*, *3*, 2004, 2405–2411.

[15] H. Herr and M. Popovic, Angular momentum in human walking, *The Journal of Experimental Biology*, *211*(4), 2008, 467–481.

[16] A. Hofmann, M. Popovic, and H. Herr, Exploiting angular momentum to enhance bipedal center-of-mass control, *IEEE International Conference on Robotics and Automation*, 2009, 4423–4429.

[17] T. Komura, H. Leung, S. Kudoh, and J. Kuffner, A feedback controller for biped humanoids that can counteract large perturbations during gait, *IEEE International Conference on Robotics and Automation*, 2005, 1989–1995.
[18] T. Sugihara and Y. Nakamura, Whole-body cooperative balancing of humanoid robot using COG Jacobian, *IEEE/RSJ International Conference on Intelligent Robots and Systems*, *3*, 2002, 2575–2580.
[19] S.-H. Lee and A. Goswami, A momentum based balance controller for humanoid robots on non-level and non-stationary ground, *Autonomous Robots*, *33*(4), 2012, 399–414.
[20] R. Beranek, H. Fung, and M. Ahmadi, A walking stability controller with disturbance rejection based on cmp criterion and ground reaction force feedback, *IEEE/RSJ International Conference on Intelligent Robots and Systems*, 2011, 2261–2266.
[21] O. Barker, R. Beranek, and M. Ahmadi, Design of a 13 degree-of-freedom biped robot with a CAN-based distributed digital control system, *IEEE/ASME International Conference on Advanced Intelligent Mechatronics*, 2010, 836–841.
[22] I. Poulakakis and J. Grizzle, The spring loaded inverted pendulum as the hybrid zero dynamics of an asymmetric hopper, *IEEE Transactions on Automatic Control*, *54*(8), 2009, 1779–1793.
[23] T. Sugihara, Standing stabilizability and stepping maneuver in planar bipedalism based on the best COM-ZMP regulator, *IEEE International Conference on Robotics and Automation*, Kobe, 2009.
[24] B. Stephens and C. Atkeson, Push recovery by stepping for humanoid robots with force controlled joints, *IEEE International Conference on Humanoid Robots*, Nashville, 2010.
[25] J.J. Alcaraz-Jiménez, D. Herrero-Pérez, and H. Martínez-Barberá, Robust feedback control of ZMP-based gait for the humanoid robot Nao, *The International Journal of Robotics Research*, *32*(9–10), 1074–1088.

## Biographies

*Richard Beranek* received his B.Eng. degree from Carleton University, in 2009. He is currently pursuing a Ph.D. degree in mechanical engineering from Carleton University. His research interests include bipedal robot control, behaviour-based control and reinforcement learning. Richard is a student member of IEEE.

*Henry Fung* received his B.Eng. degree in 2008 and M.A.Sc. degree in 2011 from Carleton University, Canada. His focus was on bipedal robot modelling and control. From 2011 he has worked for the flight simulator manufacturer CAE Inc. in Montreal, Canada.

*Mojtaba Ahmadi* received the B.Sc. degree from Sharif University of Technology, Tehran, Iran, in 1989, the M.Sc. degree from the University of Tehran, Iran, in 1992, and the Ph.D. degree in mechanical engineering from McGill University, Montreal, Canada, in 1998. He worked on robotic teleoperation and autonomous operation as a Postdoctoral Fellow at Ecole Polytechnique de Montreal (1998–2000) and from 2000 to 2005, he held senior positions in different industries including Opal-RT Technologies Inc., Montreal, Quantum and Maxtor Corporations, San Jose, CA, and the Institute for Aerospace Research of the National Research Council Canada, Ottawa, ON, Canada. He joined the Department of Mechanical and Aerospace Engineering, Carleton University, Ottawa, in 2005, where he is currently an Associate Professor. He founded the Advanced Biomechatronics and Locomotion Lab (ABL), and his current interests include rehabilitation robotics, assistive devices, human–robot interaction, design and control of mechatronics systems and legged robots.